

# PD-1 blockade employed at the time CD8+ T cells are activated enhances their antitumor efficacy

Jena E Moseman , Ichwaku Rastogi , Donghwan Jeon, Douglas G McNeel 

**To cite:** Moseman JE, Rastogi I, Jeon D, *et al.* PD-1 blockade employed at the time CD8+ T cells are activated enhances their antitumor efficacy. *Journal for ImmunoTherapy of Cancer* 2025;**13**:e011145. doi:10.1136/jitc-2024-011145

► Additional supplemental material is published online only. To view, please visit the journal online (<https://doi.org/10.1136/jitc-2024-011145>).

Accepted 22 April 2025

## ABSTRACT

**Background** We have previously shown that immune checkpoint receptors, including PD-1, are upregulated on T cells at the time of their activation, and that blockade of these receptors can improve the efficacy of antitumor vaccines. In the present study, we sought to determine whether, and by what mechanisms, the timing of PD-1 blockade with respect to vaccination affects antitumor T cell function.

**Methods** TRAMP-C1 or E.G7-OVA tumor-bearing mice received PD-1 blockade at different timing intervals with a tumor-associated antigen vaccine. Tumor growth, survival, and immune-infiltrating populations were assessed. In vitro models of T cell activation using OT-I T cells and PD-(L)1 axis disruption with a PD-1 blocking antibody or PD-L1<sup>KO</sup> dendritic cells were used.

**Results** Mice receiving PD-1 blockade at the time of T cell activation with vaccine had better antitumor outcomes in comparison to mice receiving PD-1 blockade before or after immunization. T cells activated in vitro in the presence of PD-(L)1 axis disruption had a more differentiated, functional phenotype with decreased CD28 and CCR7 expression and increased production of the Tc1 cytokines IL-2, TNF $\alpha$ , and IFN $\gamma$ . Intriguingly, a small subset of undifferentiated cells (CD28+) was of a stem-like Tc17 phenotype (IL-17 $\alpha$ +, TCF1+). Tumor-bearing mice receiving T cells activated in the presence of PD-(L)1-axis disruption had better antitumor outcomes and a greater number of complete responses.

**Conclusions** These data indicate that PD-1 blockade, when used with antitumor vaccines, acts primarily at the time of T cell activation, not exclusively within the tumor microenvironment. Consequently, PD-1 blockade may be best used when delivered concurrently with T cell activating agents such as vaccines.

## BACKGROUND

The field of cancer immunotherapy has been accelerated by the discovery of immune checkpoint blocking antibodies. These therapies work by blocking the negative interaction between T cell checkpoint receptors and their ligands. Checkpoint ligands are upregulated on tumor cells due to a variety of tumor intrinsic or extrinsic factors but are also upregulated in certain conditions on immune cells such as antigen-presenting cells in the presence of interferons or other cytokines.<sup>1</sup> These

## WHAT IS ALREADY KNOWN ON THIS TOPIC

⇒ We previously found immune checkpoint receptors on CD8+ T cells were upregulated after vaccination, and blockade of these receptors at the time of vaccination improved antitumor outcomes. Therefore, we sought to determine whether differences in timing of PD-1 blockade with T cell activation affected antitumor immunity and whether this was acting at the time of T cell activation or within the tumor microenvironment, using model antigen systems and mouse models of prostate cancer.

## WHAT THIS STUDY ADDS

⇒ This study determined that PD-(L)1-axis disruption at the time of T cell activation resulted in CD8+ T cells with distinct phenotypic and functional profiles, which resulted in improved antitumor outcomes.

## HOW THIS STUDY MIGHT AFFECT RESEARCH, PRACTICE OR POLICY

⇒ Results from this study may inform decisions regarding the sequencing or delivery methods of combination immunotherapies consisting of T cell activating agents and immune checkpoint blockade.

immune checkpoint blocking therapies have proven to be very successful in several disease types such as melanoma, Merkel cell carcinoma, non-small cell lung cancer (NSCLC), renal cell cancer, urothelial cancer, and head and neck cancers.<sup>2</sup> The wide success of these agents to prolong survival has led to the approval by the United States Food and Drug Administration (FDA) of PD-1 blocking antibodies and PD-L1 blocking antibodies for these diseases. In 2023, the FDA approved the use of a PD-1 blocking antibody, pembrolizumab, in any metastatic or unresectable solid tumor that is mismatch repair deficient (dMMR) or microsatellite instability-high (MSI-H) that has failed to respond to other treatments.

Prostate cancer, the second-leading cause of cancer-related death in men in the USA, is generally considered an “immunologically cold” tumor, with few infiltrating lymphocytes.



© Author(s) (or their employer(s)) 2025. Re-use permitted under CC BY-NC. No commercial re-use. See rights and permissions. Published by BMJ Group.

University of Wisconsin-Madison Carbone Cancer Center, Madison, Wisconsin, USA

## Correspondence to

Dr Douglas G McNeel;  
dm3@medicine.wisc.edu

Only 1%–5% of patients with advanced prostate cancer have dMMR and/or MSI-H tumors.<sup>3,4</sup> Consequently, the use of PD-1 blocking antibodies and other immune checkpoint blockade has demonstrated little activity when used alone as treatment for prostate cancer.<sup>5,6</sup> Notwithstanding, sipuleucel-T, an autologous cellular cancer vaccine, received FDA approval for metastatic prostate cancer in 2010 based on clinical trials showing median survival improvement of 4.1 months compared with placebo.<sup>7,8</sup> The FDA approval of sipuleucel-T for prostate cancer suggests the use of T cell activating therapies such as cancer vaccines may be a feasible treatment approach for this disease, and their efficacy might be improved with immune checkpoint blockade.<sup>9</sup>

We have previously demonstrated that vaccination elicited T cells with increased expression of PD-1 and other checkpoint receptors, and that blockade of these signaling axes in combination with immunization improved anti-tumor responses in mouse models of cancer and in human clinical trials.<sup>10–15</sup> In particular, in one human clinical trial of patients with prostate cancer, we demonstrated that administration of a PD-1 blocking agent after completing a vaccine course led to fewer prostate-specific antigen (PSA) declines in comparison to patients receiving PD-1 blockade concurrently with vaccination.<sup>16</sup> Additionally, others have found in mice that administration of PD-1 blockade before immunization led to an ineffective T cell response by eliciting T cells with a CD38<sup>hi</sup> dysfunctional phenotype.<sup>17</sup> These studies demonstrate the need for a better understanding of the timing required and underlying mechanisms of action of PD-1 blockade in combination with T-cell activating agents like vaccines.

In the present study, we hypothesized that the timing of PD-(L)1-axis blockade with respect to T cell activation could either affect CD8<sup>+</sup> T cell function and antitumor immunity directly, or by protecting PD-1-expressing activated CD8<sup>+</sup> T cells from PD-L1 ligation in the tumor immune microenvironment. Using E.G7-OVA-PD-L1<sup>hi</sup> and TRAMP-C1 tumor models, we assessed whether the timing of PD-1 blockade either before, simultaneously, or after immunization affected tumor growth and survival outcomes. Using in vitro models of T cell activation, we assessed whether T cell transcriptome and secretome profiles were affected by PD-1 blockade when employed at the time of T cell activation.

## MATERIALS AND METHODS

### Mice

C57Bl/6J (B6, Cat. #000664), OT-I (Cat. #003831), PD-L1<sup>Flox/Flox</sup> (Cat. #036255), CD11c-Cre (Cat. #008068), and CD45.1 “JaxBoy” (C57BL/6J-*Ptprc*<sup>em6Lutz</sup>/J, Cat. #033076) mice were purchased from Jackson Labs (Bar Harbor, ME). PD-L1<sup>KODC</sup> mice were generated as previously described.<sup>18</sup> Briefly, PD-L1<sup>F/F</sup> mice were bred to CD11c-Cre mice. Resulting PD-L1<sup>F/wt</sup>.CD11cCre+pups were backcrossed to generate PD-L1<sup>F/F</sup>.CD11cCre+mice (hereafter referred to as PD-L1<sup>KODC</sup> mice). All mice

were maintained in aseptic conditions under an IACUC-approved protocol.

### Cell lines

E.G7-OVA (derivative of EL4) was obtained from ATCC (Manassas, VA, Cat #CRL-2133) and lentivirally transduced to express high levels of PD-L1, as previously described<sup>12</sup> (hereafter referred to as “E.G7”). The TRAMP-C1 cell line was obtained from ATCC. All cell lines were maintained in cell culture media recommended by ATCC. Primary mouse splenocytes and dendritic cells were cultured in mouse media consisting of RPMI-1640 with L-glutamine (Corning, Corning, NY, Cat #10040CV), 10% fetal bovine serum (FBS; Gemini, West Sacramento, CA), 50 μM β-MeOH (Sigma-Aldrich, St. Louis, MO), 1% HEPES (Cytiva, Logan, UT), 1% sodium pyruvate (Corning), and 200 U/mL pen/strep (Corning).

### Blocking antibodies

The anti-mouse PD-1 blocking antibody (Clone G4) was a gift from Dr. Lieping Chen and purified by Envigo (Madison, WI). The Armenian hamster IgG isotype control was purchased from BioXCell (Lebanon, NH Catalog #BE0091).

### In vitro assays

#### Dendritic cell generation

Wild-type B6 or PD-L1<sup>KODC</sup> were implanted with B16 melanoma tumor cells expressing FLT3L as previously described.<sup>19</sup> Spleens from tumor-bearing mice were harvested and processed with DNase and collagenase.<sup>20</sup> Dendritic cells (DCs) were isolated using PE positive selection kits (StemCell Technologies, Vancouver, BC, Catalog #17666) or Pan-DC negative selection kits (StemCell, Cat # 19863).

#### Co-culture assays

DCs were isolated as described above and co-cultured at a 1:1 ratio with OT-I CD8<sup>+</sup> T cells isolated by CD8<sup>+</sup> T cell negative selection kit (StemCell, Cat #19853). Cells were incubated in the presence of 0.1 μg/mL SIINFEKL peptide (Lifetein, Hillsborough, NJ) plus 5 μg/mL of hamster IgG or αPD-1.

### RNA sequencing

DCs (obtained by PE positive selection) and OT-I CD8<sup>+</sup> T cells (obtained by negative selection) were co-cultured in a 2:1 (DC:T) ratio in the presence of 0.1 μg/mL SIINFEKL peptide plus 5 μg/mL hamster IgG or αPD-1. CD8<sup>+</sup> T cells were reisolated by magnetic bead separation after 48 hours incubation. Pellets were resuspended in TriReagent (Zymo Research) and frozen at −80°C for later use. RNA was isolated using a Zymo RNA miniprep kit (Cat #R2050). RNA was submitted to UW Biotechnology Center and libraries were prepped according to manufacturer's instructions using the Takara Smarter Stranded Total RNA-Seq Kit v2—Pico Input Mammalian (Takara, #634414). Samples were sequenced using an Illumina NovaSeq6000 sequencer at 30 million reads per sample.

Data were analyzed using Galaxy software (UseGalaxy.org). Heat map visualization of the top 40 changed genes was generated by sorting Deseq2 outputs based on  $\log_2FC$ . Data were also analyzed using Gene Set Enrichment Analysis Software.<sup>21 22</sup>

### ELISAs

Sandwich ELISAs were performed using cell culture supernatants and purified rat anti-mouse IFN $\gamma$  (BD #551216) and biotinylated anti-mouse IFN $\gamma$  (BD #55410) along with Avidin-HRP (Biorad #170-6528) as described previously.<sup>20 23</sup>

### Luminex

Luminex assays were performed using cell culture supernatants according to the manufacturer's instructions using the ProcartaPlex Mouse Cytokine & Chemokine Panel 1, 26-plex (Invitrogen #EPXR260-26088-901). Samples were analyzed using a Luminex MAGPIX machine (ThermoFisher).

### Flow cytometry

Fc receptors were blocked with either 50% FBS/50% PBS or  $\alpha$ CD16/32 (BD, Cat #553142) for 20 min. Cells were then washed, stained for surface markers and tetramer, fixed overnight at 4°C using the eBioscience FoxP3 Fixation/Permeabilization kit (Invitrogen #00-5523-00), stained for intracellular markers, and assessed by flow cytometry on an Attune NxT flow cytometer (ThermoFisher Scientific). When intracellular cytokine staining was used, T cells were stimulated for the amount of time indicated in the figure legends, and monensin (GolgiStop, BD #554724) was added 6 hours prior to the end of incubation. The following antibodies were used: SIINFEKL tetramer BV421 (NIH tetramer facility, Atlanta, GA), CD28 BB700 (BD #566512), CCR7 BV421 (BD #562675), CD8 AlexaFluor700 (Biolegend #100730), CD3 PE-Cy5 (Biolegend #100310), CD3 PE-Cy7 (Invitrogen #25-0031-82), CD4 BV605 (Biolegend #100451), CD45 BV510 (BD #563891), CD45 PerCP-Cy5.5 (Biolegend #103132), CD19 BV711 (BD #563157), CD11c APC (BD #550261), Ghost780 (Tonbo #13-0865 T500), CD62L BV510 (Biolegend #104441), CD44 Alexa488 (Biolegend #103016), KLRG1 PE (Biolegend #138408), CD127 APC (Biolegend #121122), CD11b BB515 (BD #564454), CD25 BB700 (BD #566499), Gr-1 PE-CF594 (BD #562710), Perforin FITC (Invitrogen #11939282), IFN- $\gamma$  PE (BD #554412), TNF- $\alpha$  PECy7 (BD #557644), IL-2 APC (eBioscience #17-7021-82), Granzyme B PE-eFluor610 (Invitrogen #61-8898-82), Ki67 PE-Cy7 (BD #562899), Tcf1 PE (BD #564217), IL-17 $\alpha$  BV605 (BD #564169), CD45.2 FITC (Biolegend #109806), Perforin APC (Biolegend 154304), CD11b PECy5 (Biolegend #101210), and CD45 BV711 (Biolegend #103147). Data were analyzed using FlowJo v10 (BD, Ashland, OR).

### Tumor studies

#### Splenocyte adoptive transfer studies with E.G7 tumors

Female B6 mice, 6–8 weeks of age, were implanted with E.G7 tumors on day 0 subcutaneously. Because these

tumors have different growth rates in male and female mice, mice of only one sex (female) were used for each of these studies. When tumors were palpable, at day 9, mice received a single intraperitoneal (IP) injection containing  $2 \times 10^6$  syngeneic OT-I splenocytes. All mice received a single subcutaneous injection of 100  $\mu$ g SIINFEKL peptide in PBS on day 10. Mice received 100  $\mu$ g of  $\alpha$ PD-1 on days 8 (pre), 10 (simultaneous) or 12 (post), or IgG (100  $\mu$ g) on day 10 IP. Tumors were measured three times weekly, and tumor volumes were calculated according to the following formula:  $\frac{\pi}{6} \times (\text{short axis})^2 \times \text{long axis}$ . For all tumor growth studies, average tumor growth curves were stopped for a particular group once a single mouse in that group reached the endpoint. In addition, because there can be mild variability in tumor growth rates from one experiment to another, all tumor growth studies were performed at least twice for scientific rigor, with replicate data shown in online supplemental figures.

#### Adoptive transfer studies of OT-1 splenocytes activated in vivo in OT-1 mice

Naïve OT-1 mice were immunized with 25  $\mu$ g SIINFEKL peptide subcutaneously (or PBS control). Mice received a single IP injection of 100  $\mu$ g  $\alpha$ PD-1 either 2 days prior, simultaneously with, or 2 days postimmunization. 1 day after the “post” mice received  $\alpha$ PD-1 treatment, all mice were euthanized, and  $2 \times 10^6$  splenocytes were adoptively transferred into E.G7 OVA PD-L1<sup>hi</sup> tumor-bearing mice, 9 days post-tumor implantation. In some studies, tumor-bearing mice were congenic (CD45.1) and were euthanized on day 15 post-tumor implantation for TIL and splenocyte immunophenotyping. Tumors were harvested and digested in mouse media containing DNase, collagenase, and protease inhibitor to generate single cell suspension for flow cytometry staining of infiltrating cells.

#### Adoptive transfer of preactivated CD8+ T cells in the E.G7 tumor model

Female B6 mice, 6–8 weeks old, were implanted with E.G7 tumors on day 0 subcutaneously. When tumors were palpable, at day 9, mice received a single IP injection containing  $10^6$  reisolated OT-I CD8+T cells, which had been activated in the presence of 0.1  $\mu$ g/mL SIINFEKL peptide plus 5  $\mu$ g/mL of IgG or  $\alpha$ PD-1 for 48 hours, as described above. Mice were followed for tumor growth three times weekly. Average tumor growth curves were stopped for a particular group once a single mouse in each group reached endpoint. In some studies, mice were euthanized on day 15 post-tumor implantation, and tumors were harvested and digested in mouse media containing DNase, collagenase, and protease inhibitor to generate single-cell suspension for flow cytometry staining of infiltrating cells.

#### DNA immunization studies with TRAMP-C1 tumors

Male B6 or PD-L1<sup>KODC</sup> mice, where indicated, were implanted subcutaneously with  $10^6$  TRAMP-C1 tumor cells resuspended in 50% Matrigel/50% PBS. Beginning



on day 8, and every other week thereafter, mice were immunized intradermally in the ear pinna with 100 µg of pTVG4 (empty vector control) or pTVG-AR (a DNA vaccine encoding the ligand binding domain of the androgen receptor<sup>24</sup>). In some studies, mice were treated at different intervals intraperitoneally with 100 µg of IgG or αPD-1 at the times indicated in the study schemas. Mice were followed for tumor growth 2–3 times weekly. In some studies, mice were euthanized 43 days post-tumor implantation, and TIL and spleens were assessed for immunophenotyping as described above.

### Functional analysis of TIL

For all TIL analysis studies with intracellular cytokine staining, tumor cells were plated and activated with CD3/CD28 Dynabeads for 4 hours at 37°C in the presence of monensin. Cells were then blocked and stained as for other flow cytometry analyses described above.

### Statistics

All statistical analyses aside from RNA sequencing studies were performed using GraphPad Prism V.5 or 9.4.1. In vitro co-culture assays were analyzed using paired t-tests, where indicated. Tumor growth studies were analyzed using the linear mixed effects model, one-way analysis of variance (ANOVA), or two-way ANOVA, as indicated. Survival studies were analyzed using a two-way log-rank test. For all analyses,  $p < 0.05$  (indicated with \*) was considered statistically significant.

## RESULTS

### PD-1 blockade delivered days prior to or after immunization with a tumor-associated antigen vaccine worsened survival outcomes in comparison to concurrent checkpoint blockade with vaccine

We have previously demonstrated that patients with advanced prostate cancer receiving PD-1 blockade after completing a course of vaccination with a tumor-associated antigen vaccine had fewer PSA declines in comparison to patients receiving PD-1 blockade during the time of vaccine administration.<sup>16</sup> Therefore, we investigated whether the timing of PD-1 blockade with respect to vaccine administration affected antitumor outcomes in a mouse model of prostate cancer. TRAMP-C1 tumor cells were implanted into C57BL/6 mice. Mice were then treated with 100 µg of pTVG4 (empty vector control) or pTVG-AR (a plasmid DNA vaccine encoding the ligand binding domain of the androgen receptor<sup>24</sup>) intradermally every other week beginning on day 8 post-tumor implantation. Mice were additionally treated with 100 µg αPD-1 intraperitoneally before and with vaccine (pre), at the same time as immunization (simultaneous), 3 days post each immunization, 7 days post each immunization, or beginning at the time of the boosting dose on day 22 and simultaneously with each vaccine thereafter, as shown in the study schema in [figure 1A](#). As shown in [figure 1B,C](#) and online supplemental figures 1–3, mice

receiving PD-1 blockade either before or after vaccine administration exhibited increased tumor growth and shorter survival in comparison to mice receiving concurrent PD-1 blockade with vaccine administration. To determine whether there were differences in the tumor microenvironment or spleens of treated mice, mice were euthanized 43 days after tumor implantation. While not statistically significant, there was a trend toward increased percentages of effector CD8+TIL producing granzyme B in mice receiving vaccine and simultaneous PD-1 blockade (online supplemental figure 2D). In addition, there were greater percentages of central memory CD8+ T cells, Ki67+ (proliferating) central memory CD8+ T cells, Ki67+CD11b+myeloid and Ki67+CD11c+DCs in the spleens of mice receiving vaccine with simultaneous PD-1 blockade (online supplemental figure 2E,F).

### PD-1 blockade delivered after T cell activation in an adoptive transfer model worsened survival in mice in comparison to simultaneous therapy with SIINFEKL peptide and PD-1 blockade.

To further explore the timing of PD-1 blockade with respect to T cell activation by immunization, in which we could use a single immunization to activate tumor-specific CD8+ T cells, we used an adoptive transfer model with E.G7 tumor-bearing mice. Mice were implanted with E.G7 tumors, and tumors were permitted to grow until palpable. Mice then received an adoptive transfer of naïve OT-I splenocytes intraperitoneally. All mice were then immunized once with 100 µg SIINFEKL peptide, administered subcutaneously, the day after adoptive transfer. Mice were additionally treated with 100 µg of IgG control or αPD-1, administered intraperitoneally, either 2 days before (pre), simultaneously, or 2 days after (post) T cell activation by peptide, as depicted in the study schema in [figure 2A](#). As shown in [figure 2B,C](#) and online supplemental figure 4A, mice receiving PD-1 blockade after T cell activation by peptide immunization had greater tumor growth and significantly shorter survival. In a similar study in which vaccine activation of cells was performed in non-tumor-bearing mice, naïve OT-I mice were immunized with a low dose (25 µg) of SIINFEKL peptide subcutaneously along with pre, simultaneous, or post-treatment of 100 µg PD-1 blockade, separated by 2 days each (as shown in the study schema in [figure 2D](#)). Splenocytes were then adoptively transferred to E.G7 tumor-bearing mice. Mice receiving OT-I T cells that were treated with PD-1 blockade preimmunization or post-immunization with SIINFEKL had significantly larger tumor volumes and significantly shorter survival in comparison to mice receiving simultaneous immunization and PD-1 blockade ([figure 2E,F](#), online supplemental figure 4B). To evaluate whether the antitumor effects were mediated by endogenous or adoptively transferred cells, in a repeat study, splenocytes (OT1 CD45.2) were adoptively transferred into congenic CD45.1 tumor-bearing recipient mice (as shown in the schema in online supplemental figure 5A). Mice receiving T cells activated with simultaneous

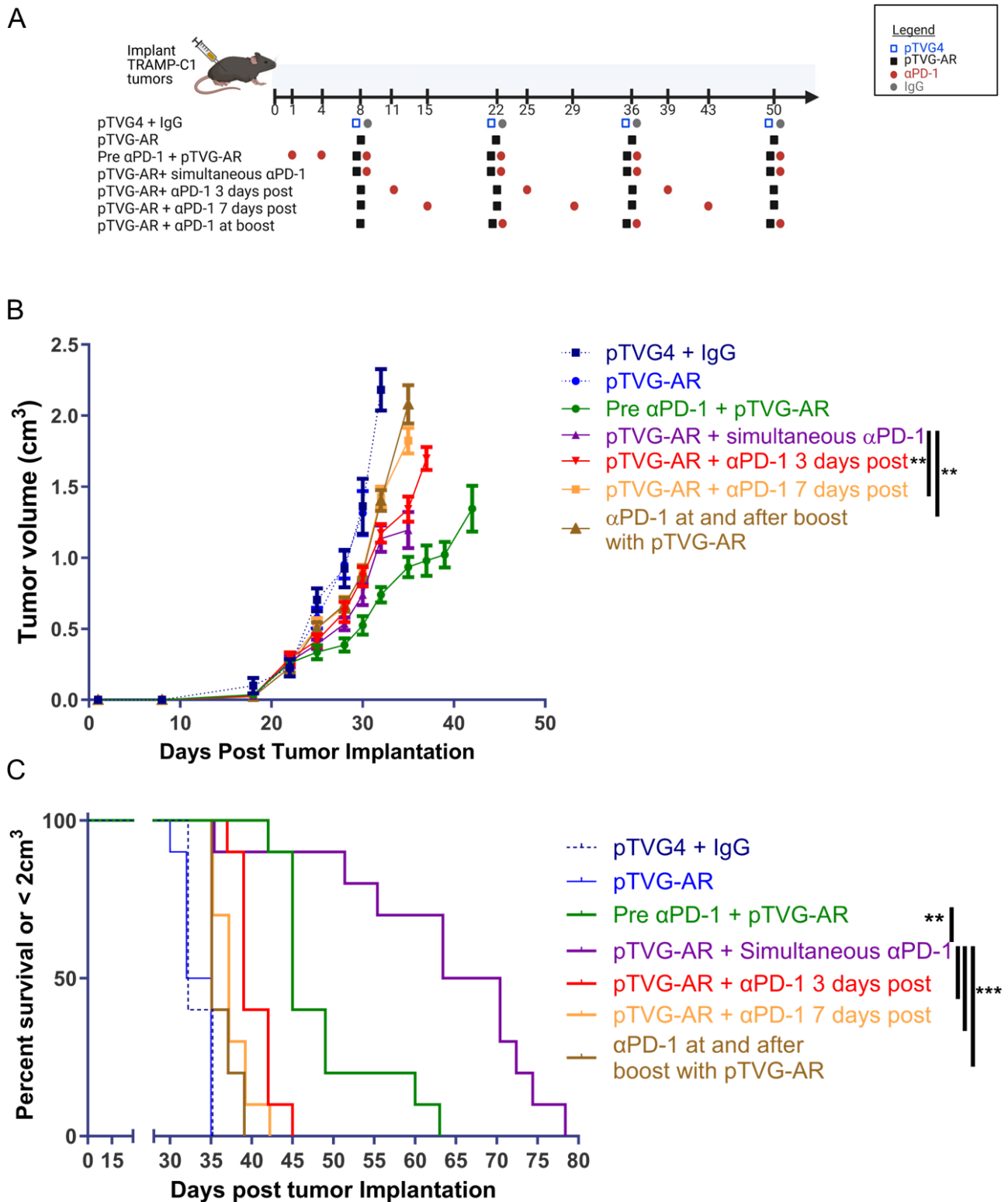


**Figure 1** PD-1 blockade delivered days prior to or after immunization with a tumor-associated antigen vaccine worsened survival outcomes in comparison to simultaneous checkpoint blockade with vaccine. (A) TRAMP-C1 tumor-bearing mice were treated biweekly intradermally with a DNA vaccine encoding the ligand-binding domain of the androgen receptor (pTVG-AR), or control DNA vector (pTVG4), in combination with intraperitoneal αPD-1, with treatment continuing until tumor size reached 2 cm<sup>3</sup> or the animal died, as indicated in the study schematic. (B) Shown are average tumor growth curves for each group until one mouse in that group reached the endpoint (n=10 animals/group). Error bars represent mean±SEM. (C) Kaplan-Meier survival curves depicting an event of death or a tumor volume of 2 cm<sup>3</sup>, whichever occurred first. P values indicated were assessed by (B) two-way ANOVA with Tukey's multiple comparisons test on day 35 or (C) log-rank (Mantel-Cox) test. \*\*p<0.01 and \*\*\*p<0.001. Individual tumor growth curves are shown in online supplemental figure 1. Similar results were found in independent experiments shown in online supplemental figures 2 and 3. ANOVA, analysis of variance.

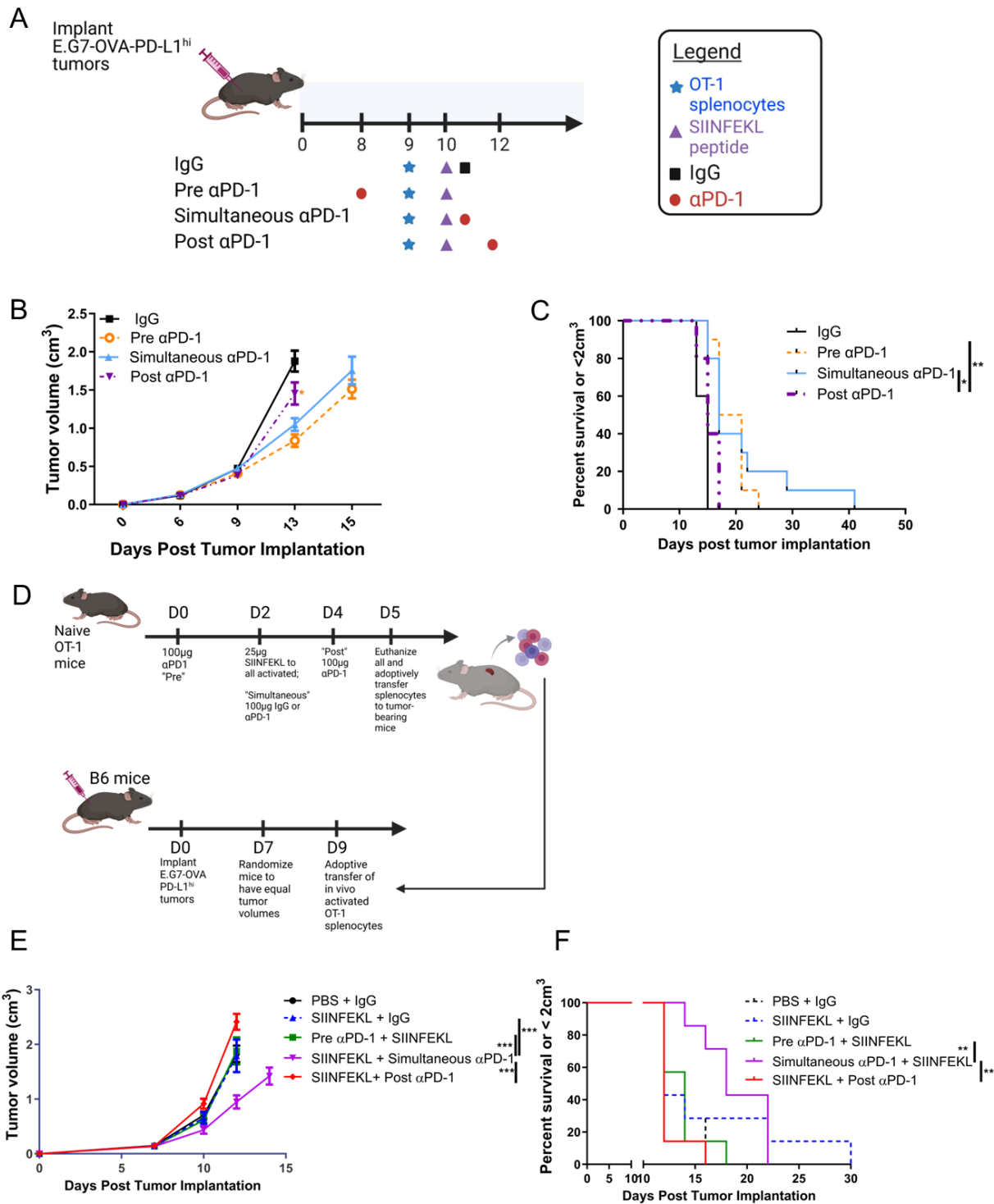


**Figure 2** PD-1 blockade delivered after T cell activation in an adoptive transfer model worsened survival in mice in comparison to simultaneous therapy with SIINFEKL peptide and PD1 blockade. (A) E.G7-OVA-PD-L1<sup>hi</sup> tumor-bearing mice received  $2 \times 10^6$  OT-I splenocytes intraperitoneally on day 9 and 100 µg of SIINFEKL peptide subcutaneously on day 10. Mice were treated with 100 µg of IgG or αPD-1 intraperitoneally on days 8 (pre), 10 (simultaneous) or 12 (post), as depicted in the schematic. (B) Shown are the tumor growth curves (mean ± SEM) until one mouse in each group reached endpoint (N=10/group). The orange asterisk represents a comparison between Pre and Post αPD-1 at day 13. (C) Kaplan-Meier survival curves depicting an event of death or a tumor volume of 2 cm<sup>3</sup>, whichever came first. P values indicated were assessed by two-way ANOVA with Bonferroni's correction (B) or log-rank test (C). \*p<0.05; \*\*p<0.01. (D–F). OT-1 mice were immunized in vivo with SIINFEKL peptide and treated with PD-1 blockade before, simultaneously, or after SIINFEKL immunization, as shown in the study schema in D. In vivo-activated OT-1 splenocytes were then adoptively transferred into CD45.1 B6 mice bearing E.G7-OVA-PD-L1<sup>hi</sup> tumors on day 9 post-tumor implantation. Shown are (E) average tumor growth curves and (F) Kaplan-Meier survival curves. P values indicated were assessed by two-way ANOVA on day 12 (E) or log-rank test (F). \*p<0.05; \*\*p<0.01; \*\*\*p<0.001. ANOVA, analysis of variance.

PD-1 blockade had slightly increased percentages of central memory and effector memory CD8+TIL (online supplemental figure 5B). Although not statistically significant, there was a trend toward increased percentages of SIINFEKL-specific adoptively transferred cells in the tumors of mice receiving simultaneous therapy (online supplemental figure 5C). However, there were also increased percentages of CD11b+, CD11c+, regulatory T cells, and myeloid derived suppressor cell (MDSC) in the TIL of mice adoptively transferred with T cells activated in the presence of PD-1 blockade (online supplemental figure 5D). Interestingly, of the adoptively transferred (CD45.2+CD8+) T cells in the spleen, mice receiving simultaneous therapy-activated T cells had increased percentages of IFN $\gamma$ +, IFN $\gamma$ +TNF $\alpha$ +, granzyme B+, and granzyme B+perforin+ cells (online supplemental figure 5E), indicating the adoptively transferred cells in this treatment group may be more functional; however, these populations were not observed at higher frequencies in the tumors (data not shown).

#### **Mice receiving CD8+ T cells activated in the presence of PD-1 blockade had reduced tumor growth and exhibited changes in the tumor immune microenvironment**

Given that mice receiving PD-1 blockade after T cell activation by vaccine exhibited diminished antitumor effects, we reasoned that PD-1 blockade may either affect the functional phenotype of T cells when employed during their activation, or that it may act on activated CD8+ T cells to protect them from PD-L1 ligation in the tumor microenvironment. Hence, we next investigated whether T cells activated *ex vivo* in the presence of PD-1 blockade, or at a later time after activation, could affect antitumor immunity on adoptive transfer into tumor-bearing mice. Mice were implanted with E.G7 tumors, and tumors were allowed to grow until palpable. On day 9, mice received adoptive transfer of OT-I CD8 T cells that had been activated for 48 hours in the presence of DCs and SIINFEKL peptide, and with IgG or  $\alpha$ PD-1 antibody (OVA- $\alpha$ PD-1 simultaneous). A third group of cells was activated for 46–48 hours with DCs and peptide and then received  $\alpha$ PD-1 for 0–2 hours immediately prior to adoptive transfer (OVA- $\alpha$ PD-1 late). As shown in [figure 3A](#) and online supplemental figure 6, mice receiving CD8+ T cells activated for 48 hours in the presence of PD-1 blockade, but not with PD-1 blockade given to CD8+ T cells after activation and prior to adoptive transfer, exhibited reduced tumor growth. In a parallel study, mice were treated as above and euthanized on day 15 post-tumor implantation. Tumor-infiltrating lymphocytes were assessed by flow cytometry. Mice receiving T cells activated in the presence of simultaneous PD-1 blockade had greater percentages of infiltrating SIINFEKL-specific CD8+ T cells in comparison to mice receiving T cells activated in the presence of late PD-1 blockade ([figure 3B](#)). As shown in [figure 3C](#), tumor-infiltrating SIINFEKL-specific CD8+ T cells were primarily of the effector-memory phenotype. Mice receiving T cells activated in the presence of

simultaneous PD-1 blockade also had greater percentages of infiltrating CD4+T cells, but no significant changes in infiltrating Treg ([figure 3D](#)). As shown in [figure 3E](#), mice receiving CD8+ T cells activated in the presence of late PD-1 blockade had increased percentages of infiltrating B cells in comparison to mice receiving IgG or simultaneous PD-1 blockade. There were no significant changes in the percentages of infiltrating monocytes (CD11b+), DCs (CD11c+), or MDSC (CD11b+, Gr1+).

#### **CD8+ T cells activated *in vitro* in the presence of PD-1 blockade had differences in gene expression and viability**

Due to the striking differences in antitumor immunity between mice receiving T cells activated in the presence of simultaneous versus late PD-1 blockade, we hypothesized that PD-1 blockade during activation of T cells affected their function and transcriptional profile. OT-I CD8+ T cells were activated in the presence of DCs, SIINFEKL peptide, and IgG or  $\alpha$ PD-1 for 48 hours. CD8+ T cells were reisolated and evaluated for gene expression changes by RNA sequencing. Shown in [figure 4A](#) is a heat map of the top 40 upregulated or downregulated genes. Surprisingly, CD28 was one of the most highly downregulated genes. Gene set enrichment analysis revealed a positive correlation with gene sets related to cyclic GMP binding ([figure 4B](#)). These results led us to investigate whether cells activated in the presence of PD-1 blockade were less apoptotic.<sup>25</sup> As shown in [figure 4C,D](#), cells activated in the presence of early PD-1 blockade were less apoptotic and had greater viability.

#### **Cells activated in the presence of PD-1 blockade exhibited differences in effector-memory phenotype and secreted cytokines**

Given that CD8+ T cells activated in the presence of PD-1 blockade had a decrease in CD28 gene expression, we hypothesized these cells may have had a more differentiated phenotype and greater effector function. Hence, OT-I CD8+ T cells were activated in the presence of SIINFEKL peptide, DCs, and IgG or  $\alpha$ PD-1 for 24–48 hours and assessed for memory phenotype by flow cytometry and secreted cytokines by Luminex. As shown in [figure 5A](#), OT-I CD8+ T cells activated in the presence of PD-1 blockade had an increased percentage of effector-memory phenotype cells. As shown in [figure 5B](#), these CD8+ T cells also had reduced expression of the differentiation markers CD28 and CCR7. CD8+ T cells activated in the presence of PD-1 blockade had an increased percentage of CD8+ T cells producing both IL-2 and TNF- $\alpha$ , as detected by flow cytometry ([figure 5C](#)). Secretion of granzyme B and/or perforin, as detected by flow cytometry, was not significantly increased (data not shown). As shown in [figure 5D](#), these cells also secreted significantly greater levels of IFN $\gamma$ , granulocyte-macrophage colony stimulating factor (GM-CSF), IL-9, IL-27, IL-23, and IL-17 $\alpha$ . Cells activated in the presence of PD-1 blockade had slightly, but not significantly, increased levels of TNF $\alpha$ , IL-1 $\beta$ , IL-10, IL-2, IL-13, IL-12p70, and IL-18, with no changes in the levels

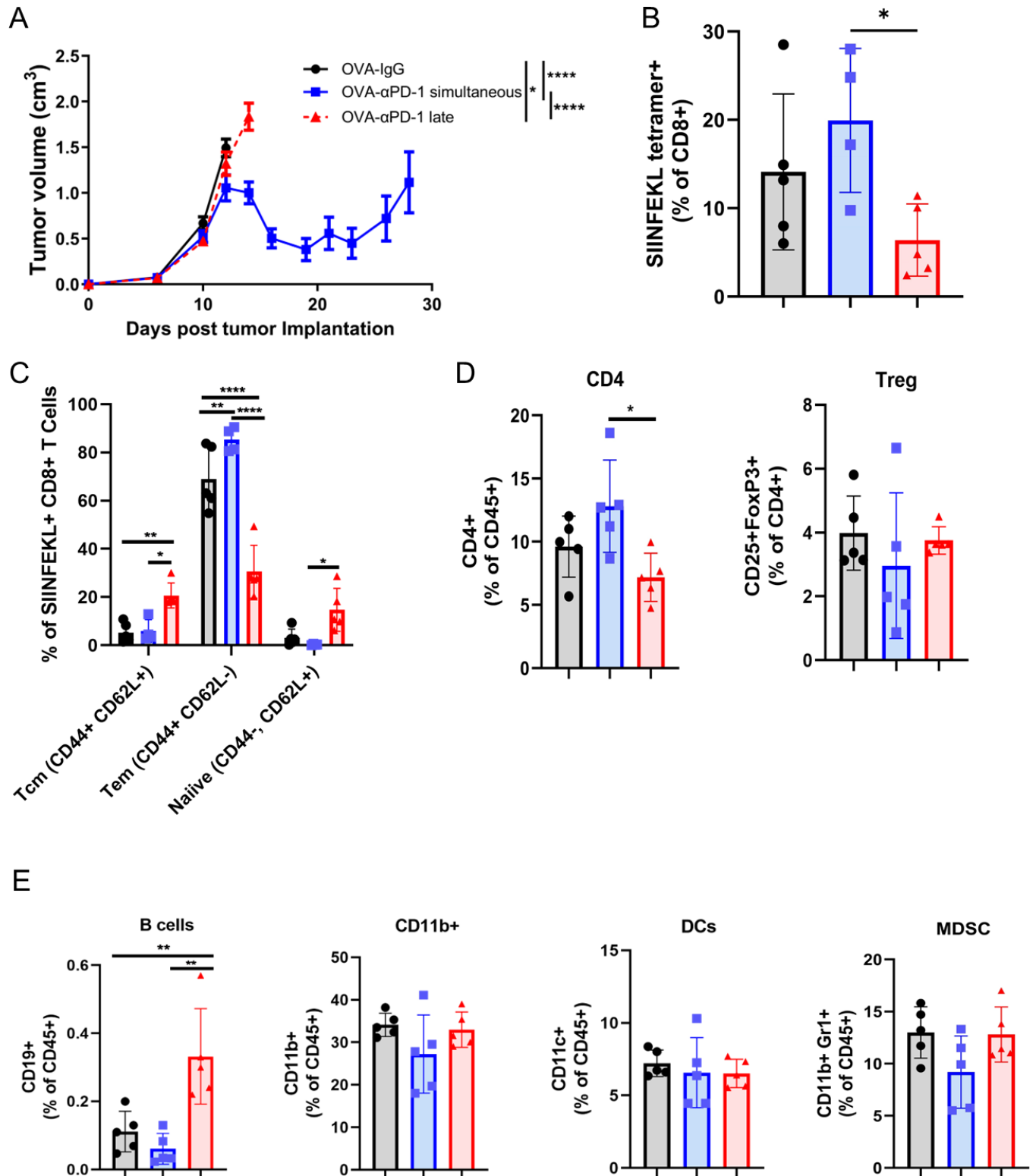


**Figure 3** Mice receiving CD8<sup>+</sup> T cells activated in the presence of PD-1 blockade had reduced tumor growth and exhibited changes in the tumor immune microenvironment. (A) OT-I CD8<sup>+</sup> T cells were isolated and activated in the presence of dendritic cells (DCs), 0.1  $\mu$ g/mL SIINFEKL peptide, and 5  $\mu$ g/mL of IgG or  $\alpha$ PD-1 for 48 hours (simultaneous) or with 5  $\mu$ g/mL  $\alpha$ PD-1 added during the last 2 hours of culture (late).  $1 \times 10^6$  reisolated CD8<sup>+</sup> T cells were adoptively transferred into E.G7-OVA-PD-L1<sup>hi</sup> tumor-bearing mice intraperitoneally on day 9. Shown are average tumor growth curves (A) and tumor-infiltrating populations on day 15 post-tumor implantation (B–E). Error bars represent mean  $\pm$  SEM from N=10 mice (A) or mean  $\pm$  SD from N=4–5 mice (B–E). P values indicated were assessed by mixed-effects model with Tukey's correction (A), one-way ANOVA with Bonferroni's correction (B–D), or two-way ANOVA with Bonferroni's correction (E). \*p<0.05; \*\*p<0.01, \*\*\*\*p<0.0001. All comparisons that were statistically significant in (B–E) are shown. Results are from one experiment and are representative of one replicate experiment. ANOVA, analysis of variance; MDSC, myeloid derived suppressor cell.



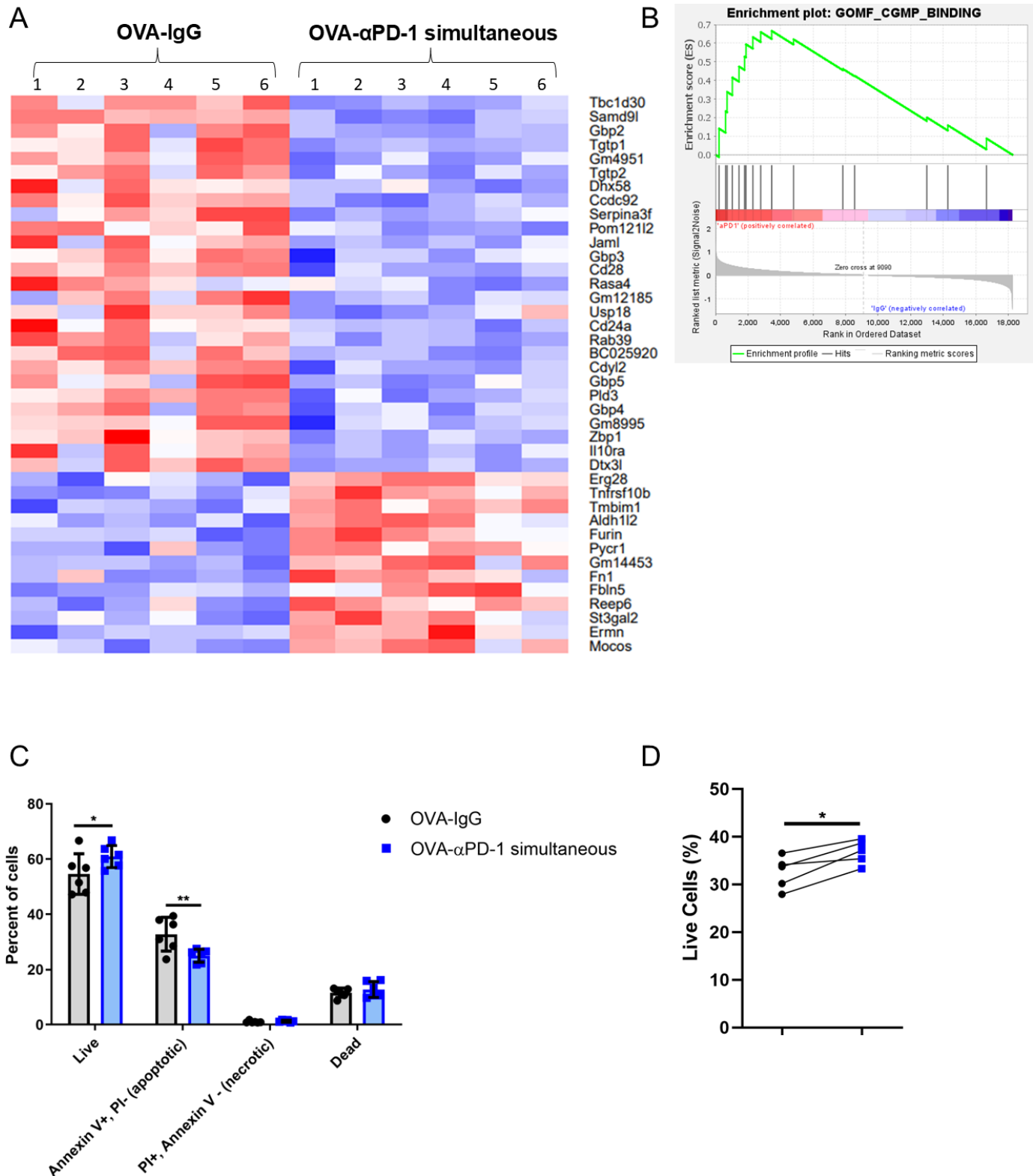


**Figure 4** CD8<sup>+</sup> T cells activated in vitro in the presence of PD-1 blockade had differences in gene expression and viability. (A). OT-I CD8<sup>+</sup> T cells were isolated and activated in the presence of dendritic cells, 0.1  $\mu$ g/mL SIINFEKL peptide, and 5  $\mu$ g/mL of IgG or  $\alpha$ PD-1 for 48 hours. CD8<sup>+</sup> T cells were reisolated and assessed for gene expression analysis by RNA sequencing. Shown is a heat map of the top 40 upregulated or downregulated genes (A) and GSEA analysis of CGMP binding (B). (C,D) Co-cultured cells were analyzed by flow cytometry for (C) early apoptosis by Annexin and Propidium Iodide staining 3 hours after activation and (D) the percentage of live cells after 48 hours incubation. P values indicated were assessed by two-way ANOVA with Bonferroni's correction (C) or Student's t-test (D). \* $p < 0.05$ ; \*\* $p < 0.01$ . ANOVA, analysis of variance; CGMP, cyclic GMP; GSEA, Gene set enrichment analysis.

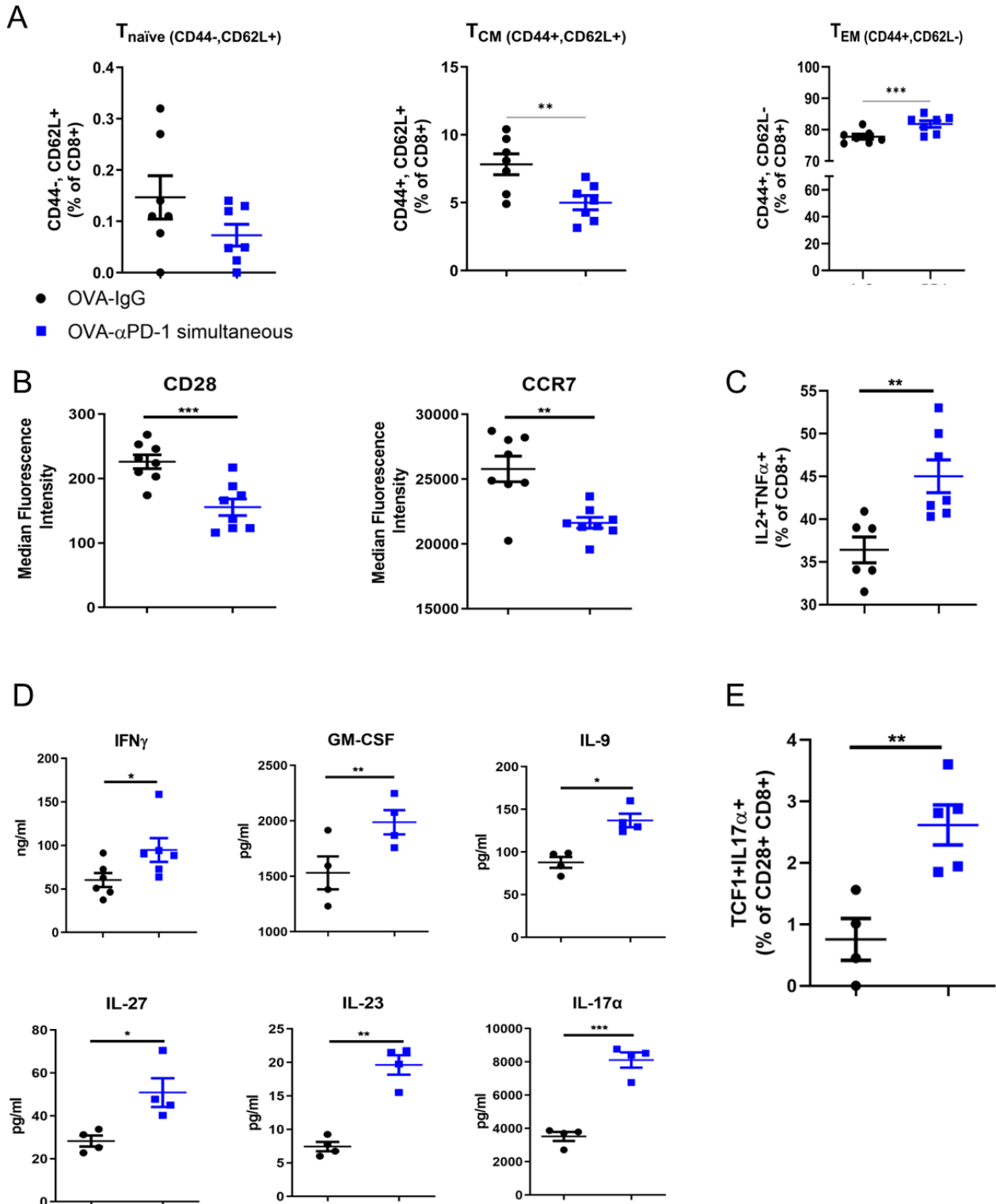


**Figure 5** Cells activated in the presence of PD-1 blockade exhibited differences in effector-memory phenotype and secreted cytokines. OT-I CD8<sup>+</sup> T cells were isolated and activated in the presence of dendritic cells, 0.1  $\mu$ g/mL SIINFEKL peptide, and 5  $\mu$ g/mL of IgG or  $\alpha$ PD-1 for 24–48 hours. (A) CD8<sup>+</sup> T cells were assessed by flow cytometry for naïve, central memory ( $T_{CM}$ ), and effector memory ( $T_{EM}$ ) phenotype on the basis of CD44 and CD62L expression. (B) CD8<sup>+</sup> T cells were assessed for CD28 and CCR7 expression levels on CD8<sup>+</sup> T cells by flow cytometry 24 hours after activation. (C) CD8<sup>+</sup> T cells were assessed for production of IL-2 and TNF- $\alpha$  24 hours after activation by flow cytometry, in the presence of monensin for the last 6 hours. (D) Frozen supernatants from cells activated for 48 hours in the presence of IgG or PD-1 blockade were assessed for cytokine secretion by ELISA or Luminex. (E) CD28<sup>+</sup>CD8<sup>+</sup> T cells were assessed for the percentage of TCF1+IL-17 $\alpha$ <sup>+</sup> cells 24 hours after activation in the presence of monensin for the last 6 hours. Error bars represent mean $\pm$ SD from N=4–8 mice. P values indicated were assessed by paired Student's t-tests. Results are from one experiment with four biological replicates (D) or representative of 1–2 additional experiments (A–C, E). \* $p$ <0.05; \*\* $p$ <0.01, \*\*\* $p$ <0.001.

of IL-5 or IL-6 as measured by Luminex (data not shown). Due to the secretome profile of these cells, we hypothesized these cells were developing a Tc17-like phenotype with self-renewing capabilities.<sup>26</sup> However, since many of the cells activated in the presence of simultaneous  $\alpha$ PD-1 have decreased expression of CD28, suggesting a more differentiated cell type, we hypothesized the Tc17-like cells (characterized by coexpression of IL-17 $\alpha$  and Tcf1) would only be present in the undifferentiated (CD28+) population. As shown in [figure 5E](#), undifferentiated CD8+ T cells (CD28+) present following activation and PD-1 blockade had increased percentages of IL-17 $\alpha$ +TCF1+cells.

### CD8+ T cells activated in the presence of PD-L1<sup>KO</sup> DCs had differences in differentiation phenotype and anti-tumor efficacy

Results from the studies above suggested that the difference in effector function of CD8 T cells activated with concurrent PD-1 blockade was due to differences at the time of T cell activation, rather than PD-1 blockade “coating” PD-1-expressing activated CD8 T cells and preventing them from being dysregulated following PD-L1/PD-1 ligation in the tumor immune microenvironment. Hence, we next focused on the interaction of PD-1 on CD8 T cells with other cells expressing PD-L1 at the time of T cell activation. Others have established the importance of PD-L1 on DCs for the efficacy of checkpoint blockade therapy.<sup>27,28</sup> Given this, we hypothesized that disruption of the PD-(L)1 axis by eliminating PD-L1 on the DCs presenting the vaccine antigen, rather than from PD-L1 expressed on other T cells, was responsible for the differences in CD8+ T cell phenotype and function. DCs were generated from wild-type mice or PD-L1<sup>KODC</sup> mice.<sup>18</sup> OT-I CD8+ T cells were activated in the presence of SIINFEKL peptide presented by wild-type DC or PD-L1<sup>KODC</sup> for 24 hours and assessed for phenotype by flow cytometry. As shown in [figure 6A](#), OT-I CD8+ T cells activated in the presence of PD-L1<sup>KO</sup> DC had significantly reduced expression levels of CD28 and slightly reduced expression levels of CCR7 ( $p=0.1152$ ). As shown in [figure 6B](#), OT-I CD8+ T cells activated in the presence of PD-L1<sup>KO</sup> DC had greater percentages in cells producing both IL-2 and TNF- $\alpha$ , and an increased percentage of cells producing IFN- $\gamma$ . There was a slight but not statistically significant increase in the percentage of CD28+cells of the TCF1+IL17 $\alpha$ +phenotype ([figure 6C](#)). Given these differentiation and functional profiles, we wanted to determine whether CD8+ T cells activated in vitro by PD-L1<sup>KO</sup> DC could affect antitumor responses. Similar to previous studies, OT-I CD8+ T cells were activated in the presence of SIINFEKL peptide plus PD-L1<sup>KO</sup> DC or wild-type DC for 48 hours. CD8+ T cells were reisolated and adoptively transferred into E.G7 tumor-bearing mice on day 9. As shown in [figure 6D,E](#) and online supplemental figure 7, mice receiving T cells activated in the presence of PD-L1<sup>KO</sup>DC had significantly reduced tumor growth and slightly ( $p=0.08$ ) prolonged survival with a greater number of cures in comparison to mice receiving T cells

activated in the presence of wild-type DCs (cures in 4/10 mice with CD8+ T cells activated by PD-L1<sup>KO</sup>DC vs 1/10 mice with CD8+ T cells activated by WT DC).

### Tumors in mice lacking PD-L1 on DCs had reduced growth following immunization with a tumor-associated antigen in comparison to wild-type mice

We next sought to determine whether mice lacking PD-L1 on DCs had a greater response to a tumor-associated antigen immunization in a relevant model of murine prostate cancer. Age-matched mice (either B6 or PD-L1<sup>KODC</sup>) were implanted with TRAMP-C1 tumors and immunized intradermally with pTVG4 or pTVG-AR every other week beginning on day 8. As shown in [figure 7A–C](#) and online supplemental figure 8, PD-L1<sup>KODC</sup> mice receiving a tumor-associated antigen immunization had significantly reduced tumor growth ( $p<0.05$ ) and slightly prolonged survival ( $p=0.09$ ) in comparison to wild-type mice receiving vaccine. There were no significant differences in tumor growth or survival of wild-type or PD-L1<sup>KODC</sup> mice receiving the empty vector control.

## DISCUSSION

We have previously found that vaccination induces checkpoint receptor expression on CD8+ T cells, and that blockade of these receptors in combination with vaccination improves antitumor outcomes.<sup>10–13</sup> In a human clinical trial, patient outcomes were improved when PD-1 blockade was given concurrently with vaccine rather than after a series of vaccinations had ended.<sup>16</sup> Additionally, others have shown that administration of PD-1 blockade before CD8+ T cells are optimally primed leads to dysfunctional T cells with a CD38<sup>hi</sup> phenotype.<sup>17</sup> These studies led us to hypothesize that PD-1 blockade at the time of T cell activation, rather than before or after activation, would lead to better antitumor outcomes by altering the phenotype of CD8+ T cells. We found that the administration of PD-1 blockade prior to or after immunization worsened anti-tumor outcomes. Specifically, we found that blockade of PD-1 binding by PD-L1 expressed on DCs during T-cell activation led to CD28 downregulation and a more differentiated T cell phenotype with greater secretion and production of functional cytokines. This was also accompanied by an increase in a minor population of Tc17-like cells with TCF1 expression. Moreover, T cells activated by DC that did not express PD-L1 had improved antitumor outcomes. These results indicate (1) PD-1 blockade may be more effective in combination with vaccines when used at the time of antigen encounter in the vaccine-draining lymph nodes rather than when delivered systemically or just to the tumor; (2) PD-1 blockade can change the effector function of T cells; (3) CD28 expression and signaling in T cells is likely more important to the efficacy of PD-1 blockade than was previously appreciated; and (4) PD-1 blockade at the time of T cell activation may induce a subset of Tc17-like cells with self-renewing capacity.

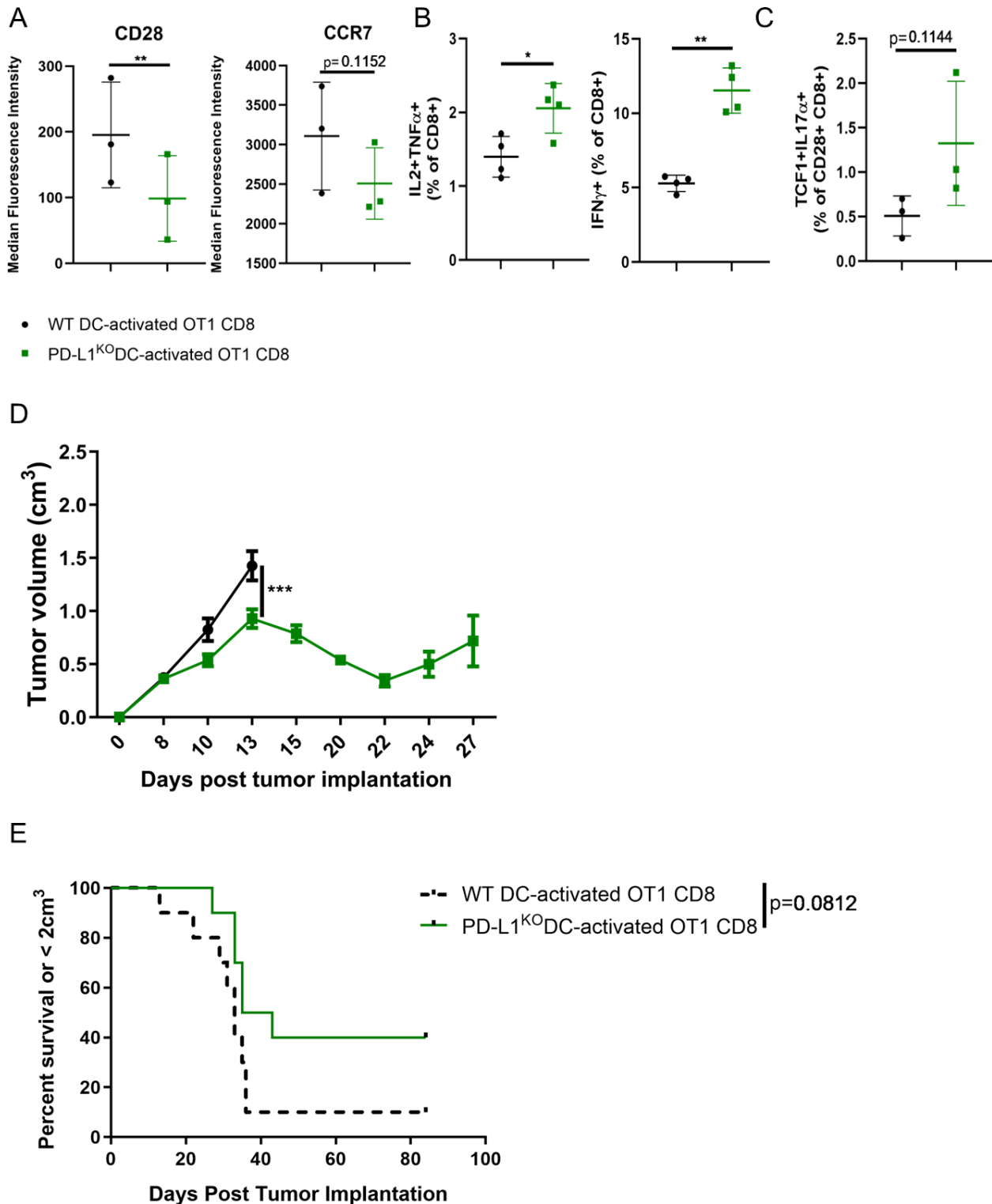


**Figure 6** Tumors in mice receiving CD8+ T cells activated in the presence of PD-L1<sup>KO</sup> DCs had reduced growth and a greater number of cures in comparison to mice receiving CD8+ T cells activated in the presence of wild-type DCs. OT-I CD8+ T cells were activated in the presence of dendritic cells from wild-type mice or PD-L1<sup>KO</sup> mice plus 0.1  $\mu$ g/mL SIINFEKL peptide for 24–48 hours. (A) CD8+ T cells were assessed for the expression of CD28 and CCR7. (B) CD8+ T cells were assessed after 24 hours, with the addition of monensin for the last 6 hours, for the production of IL-2 and TNF- $\alpha$ , or IFN- $\gamma$ . (C) CD28+CD8+ T cells were assessed for TCF1 and IL-17 $\alpha$  production 24 hours after activation, with monensin added the last 6 hours. After 48 hours of activation, CD8+ T cells were reisolated, and 10<sup>6</sup> were adoptively transferred into mice bearing E.G7-OVA-PD-L1<sup>hi</sup> tumors on day 9. Shown are (D) average tumor growth curves and (E) Kaplan-Meier survival curves. n=10 mice/group. Error bars represent mean $\pm$ SEM. P values indicated were assessed by (A–C) paired Student's t-tests, (D) two-way ANOVA with Bonferroni's correction, and (E) log-rank test. \*p<0.05; \*\*p<0.01, \*\*\*p<0.001. Results are from one experiment and are representative of one other independent experiment, shown in online supplemental figure 7. ANOVA, analysis of variance.



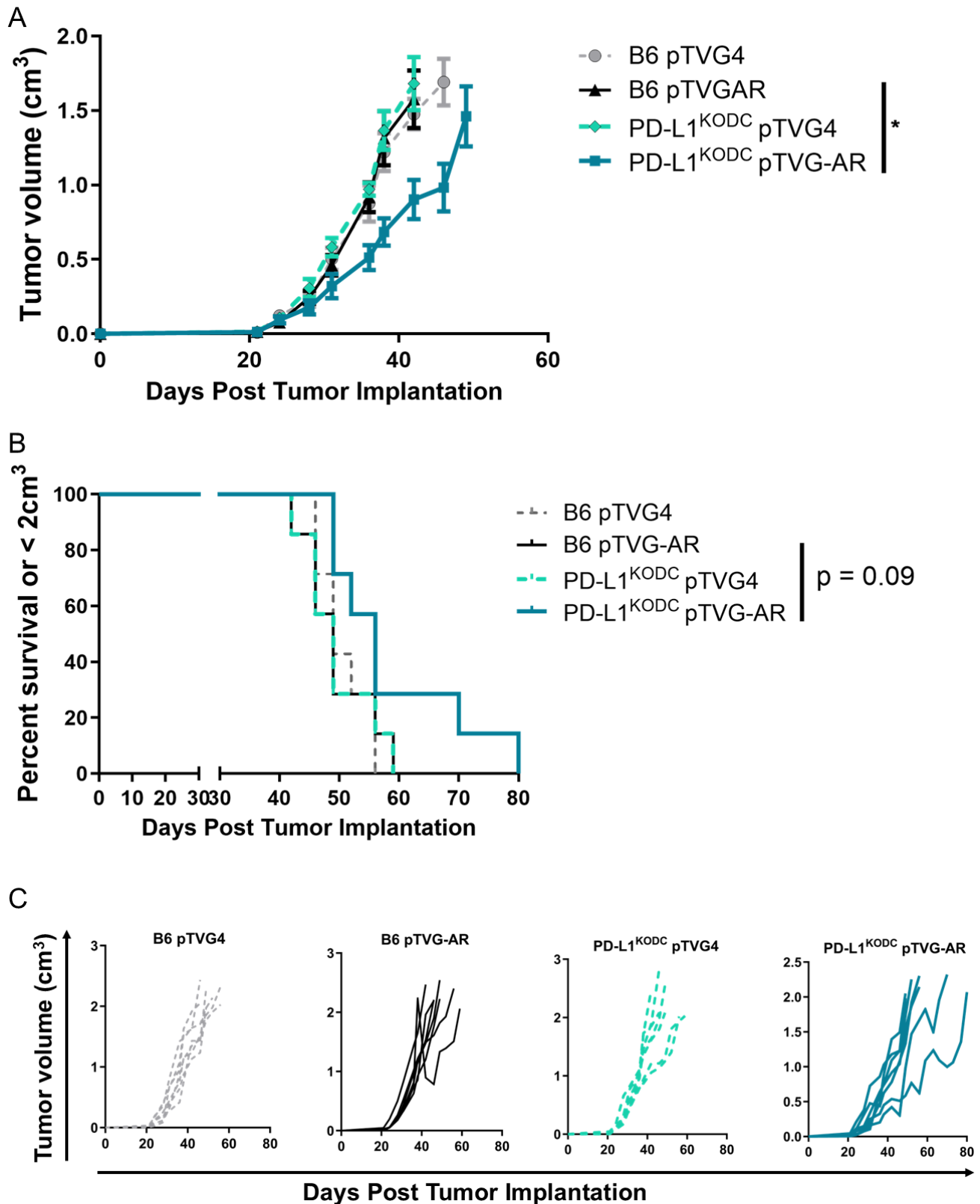


**Figure 7** Prostate tumors in mice lacking PD-L1 on dendritic cells had reduced growth following immunization with a tumor-associated antigen in comparison to wild-type mice. TRAMP-C1-bearing C57BL/6 or PD-L1<sup>KODC</sup> mice were immunized intradermally with 100 µg pTVG4 (control) or pTVG-AR (a DNA vaccine encoding the ligand binding domain of the androgen receptor) once every 14 days starting on day 8. Shown are the average tumor growth curves per group (A), Kaplan-Meier survival curves (B), and individual animal tumor growth curves (C). N=7/group. P values indicated were assessed by one-way ANOVA with Tukey's multiple comparison test (A) or by log-rank test (B). Error bars represent mean±SEM. \*p<0.05. Results are from one experiment and are representative of one replicate experiment shown in online supplemental figure 8. ANOVA, analysis of variance.

One major question in the cancer immunotherapy field is whether PD-1 blockade primarily occurs at the sites of T cell activation or primarily when T cells encounter PD-L1 in the tumor. Historically, it was well accepted that PD-L1 upregulation in the tumor microenvironment was a mechanism of immune escape.<sup>29</sup> Therefore, it was primarily thought that PD-(L)1 axis disruption primarily occurs at the site of the tumor. However, recent studies have shown that DC sources of PD-L1 were primarily responsible for the antitumor efficacy of PD-(L)1 axis inhibition, as PD-L1<sup>KODC</sup> mice showed similar tumor control to whole PD-L1<sup>KO</sup> mice, and better tumor control than macrophage PD-L1<sup>KO</sup> mice, despite macrophages being the primary source of PD-L1 in the tumor.<sup>28</sup> Another study similarly showed that tumor-bearing PD-L1<sup>KODC</sup> mice (lacking expression of PD-L1 only in DC) failed to respond to additional systemic administration of a PD-L1 blocking antibody, indicating that PD-L1 expression on DCs is largely responsible for anti-PD-(L)1 treatment efficacy. These studies also indicate PD-1 blockade may be acting to disrupt PD-(L)1-axis signaling in the tumor-draining lymph nodes (TDLN), where T cells are being activated by professional antigen-presenting cells. Indeed, several studies have shown the importance of TDLN and the response to checkpoint blockade, as removal of TDLN inhibited survival outcomes in mouse models,<sup>30</sup> and other studies showed targeted PD-L1 blockade in the TDLN prolonged survival.<sup>31</sup> These studies support our findings of the importance of the interaction between T cells and DC in PD-L1-mediated T cell inhibition, and we speculate that coadministration of PD-1 blockade along with vaccine may further improve antitumor outcomes by targeting the same antigen-presenting cell in vaccine-draining lymph nodes.

Our results indicate that T cell activation in the presence of PD-1 blockade affects T cell differentiation and function, rather than just “coating” T cells with a blocking antibody that prevents PD-L1 ligation within the tumor microenvironment. Previous studies in the early activation or reactivation setting have shown PD-(L)1 axis blockade is able to expand T cells and promote secretion of functional cytokines.<sup>27 28 32–35</sup> However, these initial studies were performed when T cells had prior access to antigen in vivo. To our knowledge, our studies are the first to show improved T cell functional response and changed differentiation status on PD-(L)1-axis blockade at the time of initial antigen encounter.

In this study, we performed bulk RNAseq on T cells activated in the presence of continuous antigen plus IgG or anti-PD-1. Although there were relatively few differentially expressed genes, interestingly, our top differentially expressed gene was CD28, which was downregulated on T cells activated in the presence of PD-1 blockade. Previous studies have demonstrated that the presence of CD28 is important for response to PD-1 blockade.<sup>36 37</sup> Kamphorst *et al* showed in a chronic viral infection model that CD28 is required to rescue exhausted CD8 T cells by PD-L1 blockade.<sup>37</sup> Additionally, CD28KO cells were unable to be

rescued by PD-L1 blockade.<sup>37</sup> Another study by Hui *et al* showed that PD-1 mediated inhibition is primarily regulated through CD28 signaling.<sup>36</sup> While our findings may seem to contradict these prior studies, we can speculate that there may be a loss of CD28 due to constant antigen stimulation and the presence of inflammatory cytokines in our system, and the majority of cells present following activation in the presence of PD-1 blockade are demonstrating a more functional but more differentiated T cell phenotype.<sup>38</sup> Further investigations into the associations between CD28 regulation and PD-1 blockade at the time T cells are activated are needed.

Although our RNA-seq studies did not reveal large differences in mRNA expression, our Luminex data showed significantly enhanced secretion of Tc17-like cytokines, namely, IL-17 $\alpha$  and GM-CSF, in addition to the Tc17-promoting cytokine IL-23.<sup>39</sup> Recent research has shown that PD-1 inhibits the ability of Tc17 cells to differentiate and produce the stemness factor TCF1.<sup>26</sup> These studies prompted us to examine IL-17 $\alpha$ +TCF1+ CD8+ T cells in our system, because Tc17 cells have been shown to be a “plastic” cell type that is able to differentiate in vivo on adoptive transfer.<sup>26 40 41</sup> We found an increase in the TCF1+IL-17 $\alpha$ +population of cells, specifically within the CD28+population, indicating we may be generating a heterogeneous population of cells that are able to initially kill the tumor, but also may be developing long-lived memory cells. Other studies have shown the importance of TCF1/*Tcf7*+stemlike cells for tumor control, as mice receiving CD8+ T cells lacking *Tcf7* had worsened survival outcomes in a tumor vaccination model.<sup>42</sup> Additionally, studies in human melanoma patients have shown an association between *Tcf7*+CD8+ cells in tumor samples and response to PD-1 blockade.<sup>43</sup> In a chronic infection model, Gill and colleagues demonstrated that PD-1 blockade led to an expansion of effector CD8+ T cells, but also expanded a smaller population of TCF1+stemlike CD8+ T cells with self-renewal capacity.<sup>44</sup> Taken together, these studies support our findings that an increase in stem-like CD8+ T cells, in addition to a more differentiated tumor antigen-specific effector T cell population, may be contributing to improved antitumor outcomes. Further research into these subsets of cells generated by PD-1 blockade-activated T cells and their cytotoxic and memory capabilities is needed.

Although we have determined the importance of timing PD-1 blockade with T cell activating agents, these studies have limitations. First, our studies primarily used ovalbumin as a model antigen for activating T cells. This allowed us to specifically isolate the events of T cell activation with a cognate antigen and PD-1 blockade, both in vitro and in vivo. However, as ovalbumin is a chicken-derived protein, and SIINFEKL has a high affinity peptide:MHC interaction, the responses demonstrated in some of these studies may be much stronger than responses that would result from T cells specific for most common shared tumor antigens. Indeed, we found that our antitumor responses in the prostate cancer model

with a shared antigen were overall less robust than in the ovalbumin studies. Additionally, these studies only focused on blocking the PD-(L)1 axis. However, we know that disrupting additional checkpoint signaling axes at the time of T cell activation may be advantageous, especially in the vaccination setting.<sup>13</sup> Overall, our studies provide evidence that PD-(L)1-axis disruption at the time of T cell activation may be important for T cell differentiation and function, and we speculate that multiple additional checkpoint blocking antibodies may be further used at the time that T cells are activated in vitro or in vivo with vaccine or other T-cell activating therapies.

**Acknowledgements** We thank the UW Biotechnology Center and UWCCC Flow Cytometry Core staff for support and technical assistance and the NIH Tetramer Facility for their support.

**Contributors** JEM designed and performed experiments, analyzed results, and wrote the manuscript; IR and DJ performed experiments; DGM oversaw the experimental design and analysis, edited the manuscript, and is responsible for the overall content as the guarantor; all authors contributed to the writing and approval of the final manuscript.

**Funding** Funding for this work was provided by NIH/NCI R01 CA219154 and to JEM by T32 CA009135.

**Competing interests** No, there are no competing interests.

**Patient consent for publication** Not applicable.

**Ethics approval** All animal studies were conducted under a University of Wisconsin-Madison Institutional Animal Care and Use Committee.

**Provenance and peer review** Not commissioned; externally peer reviewed.

**Data availability statement** Data are available on reasonable request. All data relevant to the study are included in the article or uploaded as supplementary information. The data generated and/or analyzed during this study are available from the corresponding author on reasonable request.

**Supplemental material** This content has been supplied by the author(s). It has not been vetted by BMJ Publishing Group Limited (BMJ) and may not have been peer-reviewed. Any opinions or recommendations discussed are solely those of the author(s) and are not endorsed by BMJ. BMJ disclaims all liability and responsibility arising from any reliance placed on the content. Where the content includes any translated material, BMJ does not warrant the accuracy and reliability of the translations (including but not limited to local regulations, clinical guidelines, terminology, drug names and drug dosages), and is not responsible for any error and/or omissions arising from translation and adaptation or otherwise.

**Open access** This is an open access article distributed in accordance with the Creative Commons Attribution Non Commercial (CC BY-NC 4.0) license, which permits others to distribute, remix, adapt, build upon this work non-commercially, and license their derivative works on different terms, provided the original work is properly cited, appropriate credit is given, any changes made indicated, and the use is non-commercial. See <http://creativecommons.org/licenses/by-nc/4.0/>.

## ORCID iDs

Jena E Moseman <http://orcid.org/0000-0001-6849-3225>

Ichwaku Rastogi <http://orcid.org/0000-0003-1957-1164>

Douglas G McNeel <http://orcid.org/0000-0003-1471-6723>

## REFERENCES

- Moon J, Oh YM, Ha S-J. Perspectives on immune checkpoint ligands: expression, regulation, and clinical implications. *BMB Rep* 2021;54:403–12.
- Ribas A, Wolchok JD. Cancer immunotherapy using checkpoint blockade. *Science* 2018;359:1350–5.
- Akhoundova D, Feng FY, Pritchard CC, et al. Molecular Genetics of Prostate Cancer and Role of Genomic Testing. *Surg Pathol Clin* 2022;15:617–28.
- Abida W, Cheng ML, Armenia J, et al. Analysis of the Prevalence of Microsatellite Instability in Prostate Cancer and Response to Immune Checkpoint Blockade. *JAMA Oncol* 2019;5:471–8.
- de Almeida DVP, Fong L, Rettig MB, et al. Immune Checkpoint Blockade for Prostate Cancer: Niche Role or Next Breakthrough? *Am Soc Clin Oncol Educ Book* 2020;40:1–18.
- Venkatachalam S, McFarland TR, Agarwal N, et al. Immune Checkpoint Inhibitors in Prostate Cancer. *Cancers (Basel)* 2021;13:2187.
- Kantoff PW, Higano CS, Shore ND, et al. Sipuleucel-T immunotherapy for castration-resistant prostate cancer. *N Engl J Med* 2010;363:411–22.
- Cheever MA, Higano CS. PROVENGE (Sipuleucel-T) in prostate cancer: the first FDA-approved therapeutic cancer vaccine. *Clin Cancer Res* 2011;17:3520–6.
- Rastogi I, Muralidhar A, McNeel DG. Vaccines as treatments for prostate cancer. *Nat Rev Urol* 2023;20:544–59.
- Rekoske BT, Smith HA, Olson BM, et al. PD-1 or PD-L1 Blockade Restores Antitumor Efficacy Following SSX2 Epitope-Modified DNA Vaccine Immunization. *Cancer Immunol Res* 2015;3:946–55.
- Rekoske BT, Olson BM, McNeel DG. Antitumor vaccination of prostate cancer patients elicits PD-1/PD-L1 regulated antigen-specific immune responses. *Oncoimmunology* 2016;5:e1165377.
- Zahm CD, Colluru VT, McNeel DG. Vaccination with High-Affinity Epitopes Impairs Antitumor Efficacy by Increasing PD-1 Expression on CD8<sup>+</sup> T Cells. *Cancer Immunol Res* 2017;5:630–41.
- Zahm CD, Moseman JE, Delmastro LE, et al. PD-1 and LAG-3 blockade improve anti-tumor vaccine efficacy. *Oncoimmunology* 2021;10:1912892.
- McNeel DG, Eickhoff JC, Wargowski E, et al. Phase 2 trial of T-cell activation using MVI-816 and pembrolizumab in patients with metastatic, castration-resistant prostate cancer (mCRPC). *J Immunother Cancer* 2022;10:e004198.
- McNeel DG, Emamekhoo H, Eickhoff JC, et al. Phase 2 trial of a DNA vaccine (pTVG-HP) and nivolumab in patients with castration-sensitive non-metastatic (M0) prostate cancer. *J Immunother Cancer* 2023;11:e008067.
- McNeel DG, Eickhoff JC, Wargowski E, et al. Concurrent, but not sequential, PD-1 blockade with a DNA vaccine elicits anti-tumor responses in patients with metastatic, castration-resistant prostate cancer. *Oncotarget* 2018;9:25586–96.
- Verma V, Shrimali RK, Ahmad S, et al. PD-1 blockade in subprimed CD8 cells induces dysfunctional PD-1+CD38hi cells and anti-PD-1 resistance. *Nat Immunol* 2019;20:1231–43.
- Sage PT, Schildberg FA, Sobel RA, et al. Dendritic Cell PD-L1 Limits Autoimmunity and Follicular T Cell Differentiation and Function. *J Immunol* 2018;200:2592–602.
- Kapadia D, Sadikovic A, Vanloubbeek Y, et al. Interplay between CD8α<sup>+</sup> dendritic cells and monocytes in response to Listeria monocytogenes infection attenuates T cell responses. *PLoS One* 2011;6:e19376.
- Rastogi I, McNeel DG. B cells require licensing by dendritic cells to serve as primary antigen-presenting cells for plasmid DNA. *Oncoimmunology* 2023;12:2212550.
- Mootha VK, Lindgren CM, Eriksson K-F, et al. PGC-1α-responsive genes involved in oxidative phosphorylation are coordinately downregulated in human diabetes. *Nat Genet* 2003;34:267–73.
- Subramanian A, Tamayo P, Mootha VK, et al. Gene set enrichment analysis: a knowledge-based approach for interpreting genome-wide expression profiles. *Proc Natl Acad Sci U S A* 2005;102:15545–50.
- Johnson LE, Frye TP, Chinnasamy N, et al. Plasmid DNA vaccine encoding prostatic acid phosphatase is effective in eliciting autologous antigen-specific CD8<sup>+</sup> T cells. *Cancer Immunol Immunother* 2007;56:885–95.
- Olson BM, Johnson LE, McNeel DG. The androgen receptor: a biologically relevant vaccine target for the treatment of prostate cancer. *Cancer Immunol Immunother* 2013;62:585–96.
- Shaw CA, Webb DJ, Rossi AG, et al. Cyclic GMP protects human macrophages against peroxynitrite-induced apoptosis. *J Inflamm (Lond)* 2009;6:14.
- Arra A, Lingel H, Pierau M, et al. PD-1 limits differentiation and plasticity of Tc17 cells. *Front Immunol* 2023;14:1104730.
- Peng Q, Qiu X, Zhang Z, et al. PD-L1 on dendritic cells attenuates T cell activation and regulates response to immune checkpoint blockade. *Nat Commun* 2020;11:4835.
- Oh SA, Wu D-C, Cheung J, et al. PD-L1 expression by dendritic cells is a key regulator of T-cell immunity in cancer. *Nat Cancer* 2020;1:681–91.
- Dong H, Strome SE, Salomao DR, et al. Tumor-associated B7-H1 promotes T-cell apoptosis: a potential mechanism of immune evasion. *Nat Med* 2002;8:793–800.

- 30 Fransen MF, Schoonderwoerd M, Knopf P, *et al.* Tumor-draining lymph nodes are pivotal in PD-1/PD-L1 checkpoint therapy. *JCI Insight* 2018;3:e124507.
- 31 Dammeijer F, van Gulijk M, Mulder EE, *et al.* The PD-1/PD-L1-Checkpoint Restrains T cell Immunity in Tumor-Draining Lymph Nodes. *Cancer Cell* 2020;38:685–700.
- 32 Martin-Orozco N, Wang Y-H, Yagita H, *et al.* Cutting Edge: Programmed death (PD) ligand-1/PD-1 interaction is required for CD8+ T cell tolerance to tissue antigens. *J Immunol* 2006;177:8291–5.
- 33 Goldberg MV, Maris CH, Hipkiss EL, *et al.* Role of PD-1 and its ligand, B7-H1, in early fate decisions of CD8 T cells. *Blood* 2007;110:186–92.
- 34 Tsushima F, Yao S, Shin T, *et al.* Interaction between B7-H1 and PD-1 determines initiation and reversal of T-cell anergy. *Blood* 2007;110:180–5.
- 35 Ahn E, Araki K, Hashimoto M, *et al.* Role of PD-1 during effector CD8 T cell differentiation. *Proc Natl Acad Sci U S A* 2018;115:4749–54.
- 36 Hui E, Cheung J, Zhu J, *et al.* T cell costimulatory receptor CD28 is a primary target for PD-1-mediated inhibition. *Science* 2017;355:1428–33.
- 37 Kamphorst AO, Wieland A, Nasti T, *et al.* Rescue of exhausted CD8 T cells by PD-1-targeted therapies is CD28-dependent. *Science* 2017;355:1423–7.
- 38 Mou D, Espinosa J, Lo DJ, *et al.* CD28 negative T cells: is their loss our gain? *Am J Transplant* 2014;14:2460–6.
- 39 Hipp AV, Bengsch B, Globig A-M. Friend or Foe - Tc17 cell generation and current evidence for their importance in human disease. *Discov Immunol* 2023;2:kyad010.
- 40 Lückel C, Picard FSR, Huber M. Tc17 biology and function: Novel concepts. *Eur J Immunol* 2020;50:1257–67.
- 41 Yen H-R, Harris TJ, Wada S, *et al.* Tc17 CD8 T cells: functional plasticity and subset diversity. *J Immunol* 2009;183:7161–8.
- 42 Siddiqui I, Schaeuble K, Chennupati V, *et al.* Intratumoral Tcf1+PD-1+CD8+ T Cells with Stem-like Properties Promote Tumor Control in Response to Vaccination and Checkpoint Blockade Immunotherapy. *Immunity* 2019;50:195–211.
- 43 Sade-Feldman M, Yizhak K, Bjorgaard SL, *et al.* Defining T Cell States Associated with Response to Checkpoint Immunotherapy in Melanoma. *Cell* 2018;175:998–1013.
- 44 Gill AL, Wang PH, Lee J, *et al.* PD-1 blockade increases the self-renewal of stem-like CD8 T cells to compensate for their accelerated differentiation into effectors. *Sci Immunol* 2023;8:eadg0539.